Chapter

Asphalt Fill Strengthening of Free Slip Surfaces of Shale Slopes in Asphaltite Open Quarry: Stability Analysis of Free Sliding Surface for Wet Shale Slopes in Avgamasya Asphaltite Open Quarry No 2. Site

Yildırım İsmail Tosun

Abstract

The stability analysis carried out by GEO5 software and uses free sliding analysis by wet and pore saturated weight charting provided the safety factor of 1.35. The safety precautions were followed by inclinometers and wire extensometer measurements. The other pore saturated asphalt bound shear box and unaxial test compression tests were resulted in the geotechnical and geoseismical data over sliding soil /shale inter surface quality and the characteristics of free rock falling risk and discontinuity distribution, sub crack density and distribution on stereo nets were determined. The research was firstly followed the perched water levels on geoseismical data over causing water burst or explosion of highly free mud and landslides. The hazardous rock falls over saturated soil and uncohesive rock explosions. The proposed study was secondly as strengthening methods such as asphalt mixing as precautious on shear stabilization and other wire mesh barriers anchored. The free sliding cracks was filled by asphalt and compressed for stabilization strengthening known as the characteristics of avoiding shear falls in the future. The unconditional expectations related to this study was also defined for this region such as the influence of the ground water, rock cracks and slope design, explosion exchange dynamics leading to landslide.

Keywords: mining pit, Şırnak asphaltite, free slide, landslide, mining, geoseismical analysis, stabilization, shale stability, slope stability

1. Introduction

Open pit mine slope stability and the rock fall risk assessment were studied in high steep excavation site in order to avoid landslides or rock falls occurred several times in Avgamasya Asphaltite mining sites, Şırnak. The high steep slopes were reaching over 120 m high with partly 60–65 degree shale/soil slopes developing major free landslide hazard in harsh climate conditions in recent years. The coal seam was so vertical diving at the working area of miners, made compulsory to

pre-search and take precautions by a hot melted asphalt/fly ash mixture filling through tension cracks over rock falling and free sliding cavities in the hazardous mining operation area in the open pit asphaltite mining. The critical issues and precautions for free failure in Avagamasya Open Pit Site No 2 were mentioned as below:

- Basic instability parameters searched by many researchers mentioned above anisotropy as often caused sudden failure by hazardous fractures and cracks in excavation and mining sites [1–10].

- Tensile cracks and shear loads that occurred in the free slip surfaces on heterogeneous breccias formations in Şırnak geology [11, 12] and cracks and land of asphaltite mining investigated by standards [13–16].

- Hazard risk can be examined as water income and levels in the mine [17, 18]. In the pit slopes, these values of pore pressure u are synchronized the stress and the ground water income patterns should be extracted [19, 20].

- During the works, asphalt filling stabilization of cracks on the safety of the slopes [21–24] and steps are formed in the work stages, the safety of the truck transportation road and the safety of the excavation area were ensured by anchorage reinforcement [25–29].

- A steeper safe stepping of the slopes and a suitable minimum fly ash addition pouring and crack area of asphalt filling design has been developed lower horizontal adhesive stabilization and less cracks [30–36]. High compacting vibration, drainage and low excavation capacity were also affected excavation time, free slope, crack yields and steep displacements following discontinuous failures [37, 38].

Ideally, extensometer patterns and wire cables in the stereo net were explored awareness of slide by examining the fractures in the Avgamasya asphaltite mining area. Tele monitoring of boreholes and level mirrors was made daily. In addition, acoustic sound noise analysis was also carried out. Since drilling inspection holes and daily wire follow-up was costly, taking measurements with tension wire extensometers in bevel chucks showed more reliable horizontal deformation values. Accordingly, 45 and 50 degree angles of Şırnak asphaltite quarries were found to be reliable [28, 32]. Two different design models have been developed in order to obtain these stability values. According to these models, it is thought that the slopes may be exposed to planar and wedge type shifts and frees sliding over the slip planes depending on the fracture bedding and density (**Figures 1** and **2**).

The observation of different asphaltite qualities in the field and the diversity of production provide the identification of qualified coal seams needed. Depending on the strength and hardness properties of coal, it is more difficult to determine the chemical structure and strength of asphaltites and side rocks containing heterogeneous structures compared to many other types of coal. The strength and failure type of the country rock differ. The components that make up the coal differ depending on the distribution, orientation, amount and strength and hardness values of these components in the asphaltite sample. This situation is determined relatively within a homogeneous asphaltite matrix. More qualified asphaltite shows softer mechanical strength. Hard veins are also very important in the country rocks. Asphaltite quality and development can be determined underground by seismic reflection and resistivity measurements, depending on the density **Figures 3** and **4**.

Asphaltite and shale, marly shale, marly limestone and various marly formations that are the subject of this study can also be revealed. The Siirt Formation, which is

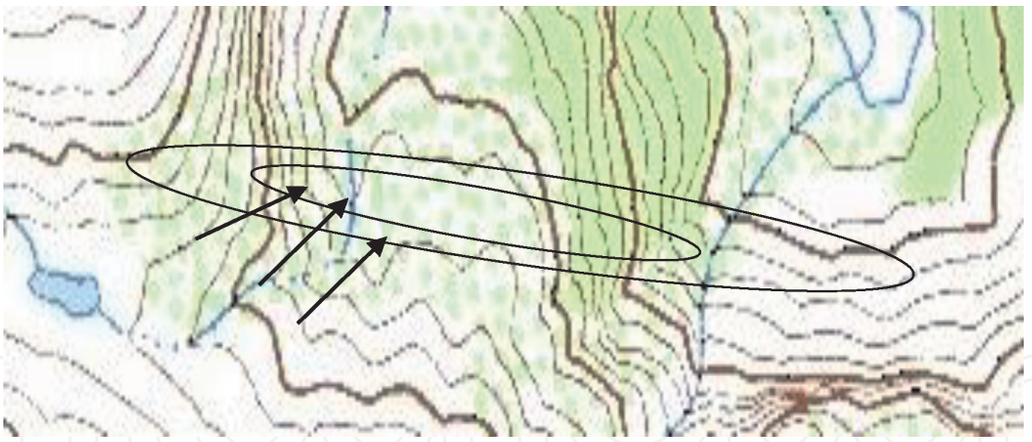

Figure 1.
Avgamasya location of Asphaltite quarry No 2 in Şırnak.

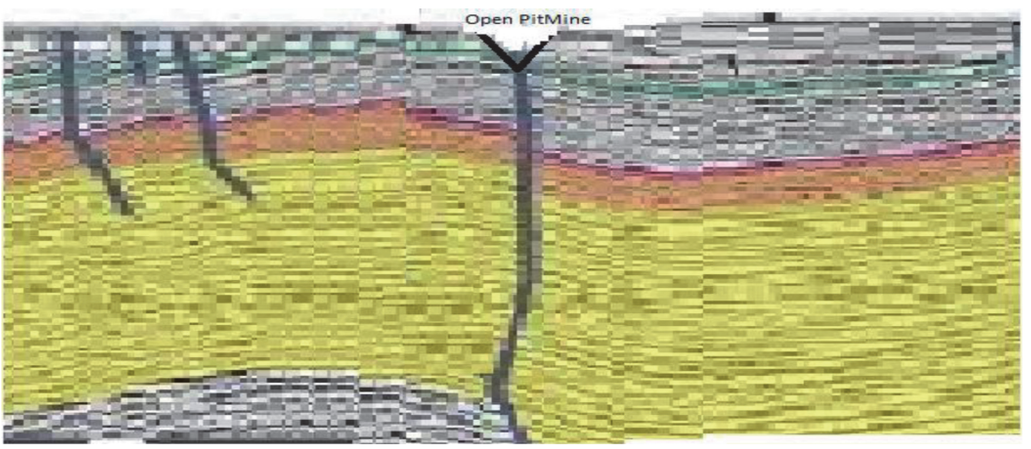

Figure 2.
Seismical formation layers of Asphaltite quarry No 2 in Şırnak.

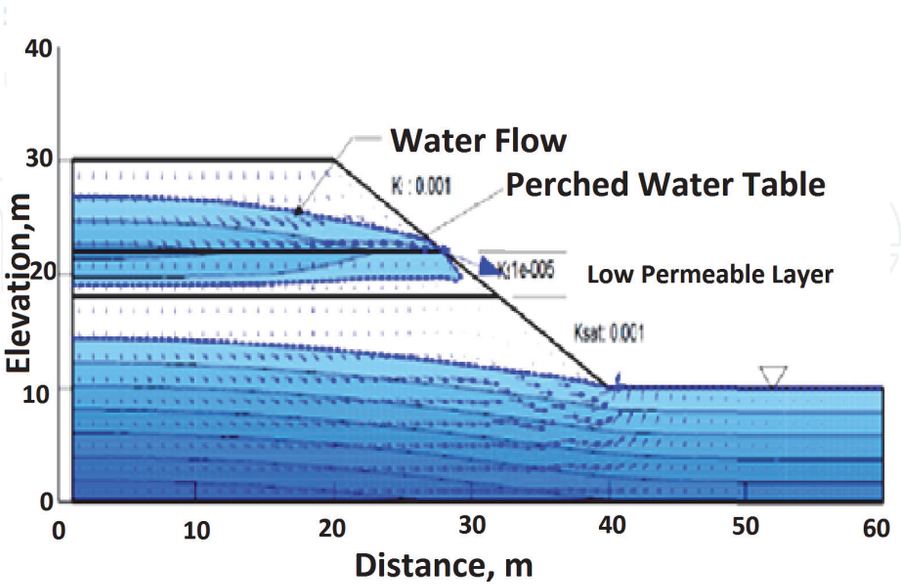

Figure 3.
S1 and S2 slope free slip surface perched water table through free slip surface.

outcropping in the west–east directions of Şırnak province, is important in bedding and forms important rock units in asphaltite bedding in terms of rock mechanics. This unit generally consists of marls containing clay and shale and clays with asphaltite. Sulphate-rich water resources are also located in these units consisting of

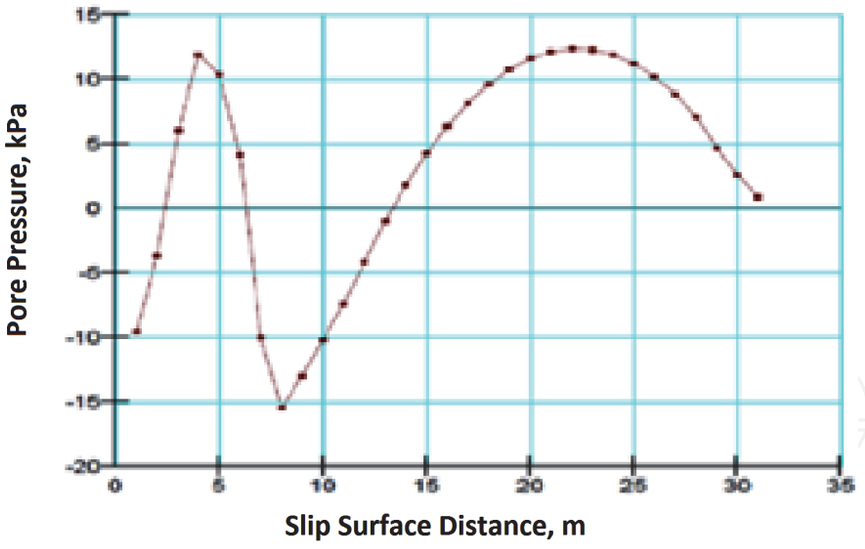

Figure 4.
S1 and S2 slope free slip surface slip surface water saturation.

claystone rocks. Due to its different mechanical strengths and densities, it helps to find underground bedding. In addition, it has been evaluated within the scope of this study since it creates various engineering data.

In operation, the drilling cores are subjected to mechanical tests on site and under laboratory conditions. The micro structural and mineralogical studies carried out. Compression tests were carried out on samples with relatively weak asphaltite and claystone levels and hard, higher strength asphaltite veins with diameters of 34 mm and 84 mm.

With the findings obtained, it was determined that asphaltites containing components with different strength and hardness properties show different fractures. It is aimed to determine the changes in different breaking stresses and strengths for each borehole and logs.

Possible bedding will be examined with seismic reflection method and exploration drillings will be opened at the location points displayed on the map below. Drilling exploration locations will be opened at 1000 m depth at the points shown on the map. Seismic reflection data describe possible asphaltite bedding as shown in the **Figure 2**.

1.1 Uniaxial compression strength tests

Uniaxial compression strength tests without environmental stress were carried out in the Şırnak University laboratory with a 2000 kN capacity hydraulic controlled test device. Axial and circumferential deformation gauges are placed at the levels of half of the sample lengths, as shown in the figure, so that their measurements are not affected by changes in the sample edges. The axial strain gauges were placed tightly on both sides of the specimens, mutually. Measuring range of axial deformation gauges on the sample is 50 mm for 84 mm diameter samples and 35 mm for 34 mm diameter samples as shown in **Figures 5** and **6**. The circumferential strain (rad) was calculated with the help of strain gauges connected to the chain wrapped around the sample. During the test (**Figure 7**), digital feedback was provided by circumferential strain and the control value used was set at 0.05 mm/min. The rock properties were defined.

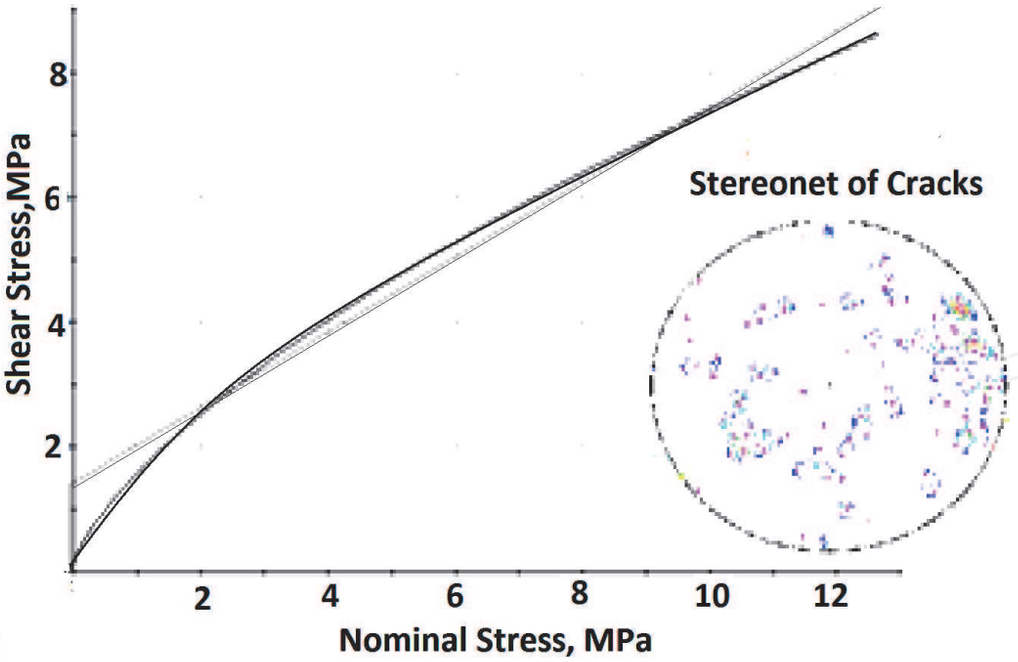

Figure 5.
Typical Mohr coulomb envelope of the Asphaltite mine shale rocks studied.

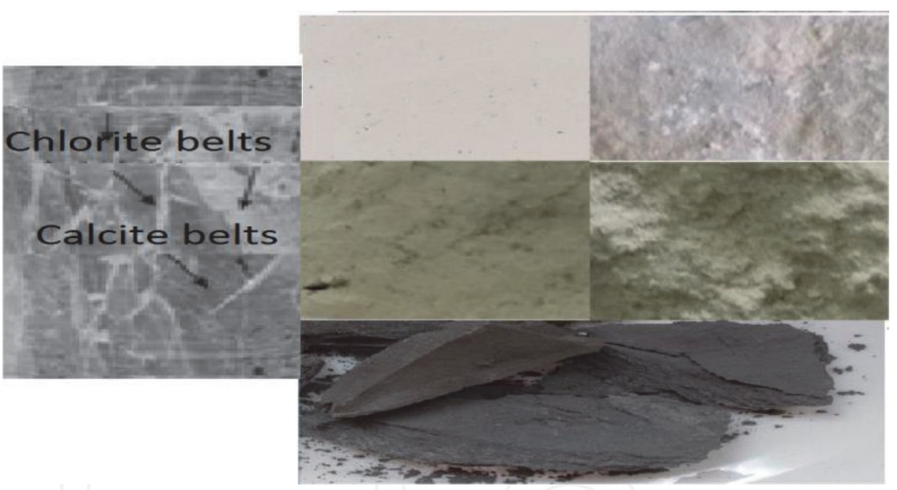

Figure 6.
Typical chlorite and calcite belts of the Asphaltite mine shale rocks studied.

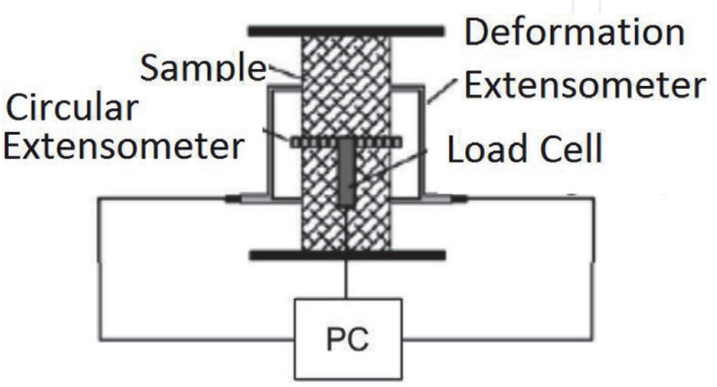

Figure 7.
Schematic view of the unaxial compression strength test setup.

2. Stability modeling and asphalt covering for free rock sliding control in Şırnak open pit coal mining

Water drained layered surfaces confirmed the geotechnical stability caused anisotrophical pore pressure developed and compression strength developed. The below equation showed the shear on fre slip surface with cohesive mater.

$$c_\theta = c_2 + (c_1 - c_2)\ \cos^2\theta \tag{1}$$

where the shear force and stress and nominal load and compression stress at angle was θ caused failure at weak layer shear in the slope.

Vertical unaxial strength and Horizontal strength of the specimens were changed.

GEO5 model weight slice chart construction carried out as given below serial equation sum:

$$F = \sum_0^{\mathrm{i}} \mathrm{N}_i \mathrm{F}_\mathrm{i} = \mathrm{N}_i \frac{C_\mathrm{i}}{\gamma H} \cos\beta^i \tag{2}$$

N_i slice load kN $\frac{C_1}{C_i}$, β slope angle, The slip surface stability analyzed as load chart sum. Safety factors over 1,35 and 1,5 was confirming the stability.

Regarding the crack distribution and density orientation and intersection with water perched tables shown (**Figure 5**) as shear risk factor $\mathrm{R}_{c.}$

10 m length slice at i discontinuity at angle of crack and density of % heteregenous distriburtion on slip surface as $\frac{dy}{dx}$ was calculated.

$$\mathrm{R}_c = \sum_0^{\mathrm{i}} \mathrm{R}_i \mathrm{F}_\mathrm{i} \tan\theta = \int_a^b e^{-ti\theta} dy^i \tag{3}$$

$$\frac{dy}{dx} = e^{-ti\theta} dy \tag{4}$$

The studied stages were as below:

Slope Stability Chart modeling was managed as shown in **Figure 3**.

The Stability mechanism and control by asphalt crack filling and cable net pillar construction was avoiding pore pressure for each slice as given Eq. (5)

$$\frac{dy}{dx} = u = \sum_0^{\mathrm{i}} \mathrm{R}_i \mathrm{F}_\mathrm{i} / \tan a \left(1 - e^{-tRi/\mu}\right)^i \tag{5}$$

u deformation intrinsic friction resistance, F weight slice, a shear fracture inclination angle t time, μ crack mud viscosity i weight slice.

The safety factor in free sliding has been investigated by following the stress cracks by transforming the slope deformations based on the internal friction angle patterns. Fracture agglomeration and cohesion-free free fall displacements can be observed above 50 mm. In order to increase the viscosity in the cracks, the waste liquid polymer materials were poured into these gaps to provide stability. The joint density over slip surface for each slice was calculated by the Equations sequentially as below:

$$\mathrm{Ji} = \sum_0^{\mathrm{i}} \mathrm{N}_i \mathrm{F}_\mathrm{i} \tan a_i \tag{6}$$

$$\mathrm{Ri} = \sum_{0}^{\mathrm{i}} \mathrm{S}_i \mathrm{W}_\mathrm{i} \cos a_i = \tag{7}$$

$$\mathrm{p_u} = \frac{\Upsilon'}{\Upsilon} \mathrm{H}_i \tag{8}$$

$$\mathrm{Fi_u} = \sum_{0}^{\mathrm{i}} \mathrm{W_i} \sin a_i - \mathrm{S}_u = \sum_{0}^{\mathrm{i}} \mathrm{W_i} - \mathrm{p_u} \tag{9}$$

$$\mathrm{S_{iu}} = \sum_{0}^{\mathrm{i}} \mathrm{c}_u{}'l \ sec\, a_i + \mathrm{Fi_u} \frac{\Upsilon'}{\Upsilon} \mathrm{H}_i \tan^2 \phi' \leq 1,25 \tag{10}$$

$$\sigma'_\theta = \sigma - u_a + \chi(u_a - u_{wi}) \tag{11}$$

$$\tau_{\theta i} = c'_i + (\sigma - u_a + \chi(u_a - u_{wi}))\ \tan\phi' \tag{12}$$

$$\mathrm{S_{iu}} = \sum_{0}^{\mathrm{i}} \mathrm{c}_u{}'l \ sec\, a_i + (\sigma - u_a + \chi(u_a - u_{wi}))\tan^2 \phi' \leq 1,25 \tag{13}$$

safety water saturated rock parameters regarding pore water content

$$\mathrm{M} = \cos a \left[1 + \frac{(\tan a \tan \phi')}{F}\right] \tag{14}$$

$$\mathrm{R_u} = \frac{\Upsilon_w{}' h_i}{\Upsilon d} \tag{15}$$

Safety factor was calculated by perched water table and water saturation

$$\mathrm{S_{Rock}} = \mathrm{S_u} \sum_{1}^{\mathrm{i}} \{[\mathrm{c'b} + (\mathrm{W_i} - ub)\tan \phi']/\cos aM\} / \sum\nolimits_{i=1}^{n} \mathrm{W}_{iu} \ sin\, a_i \tag{16}$$

$$\mathrm{S_{Rock}} = \frac{2c}{\Upsilon H} PiRi\left(\ Q_i{}' \cos\phi - R(P+S)_i/(Q_i{}' + RS_i \cot\phi)\right) \leq 1,25 \tag{17}$$

$$\mathrm{P_i} = \left\{1 - \frac{z}{H}\right\}\ \mathrm{cosec}\, \phi \tag{18}$$

$$\mathrm{Q_i} = \left\{\left[1 - \frac{z}{H}\right]^2\ \cot\phi - \cot\phi\right\} sin\phi \tag{19}$$

$$\mathrm{R} = \left(\frac{\Upsilon_w}{\Upsilon}\right)\left(\frac{z_w}{z}\right)\ \left\{\frac{z}{H}\right\} \tag{20}$$

$$\mathrm{S_i} = \left(\frac{z_w}{z}\right)\left\{\frac{z}{H}\right\}\ \sin\phi \tag{21}$$

$$\mathrm{D_i} = \left\{\left[1 - \frac{z}{H}\right]^2\ \cos\phi\right\}\ \cot\phi\ (\cot\phi\ \tan\phi - 1) \tag{22}$$

2.1 Rock texture, mineralogy and petrographic characteristics

As seen in **Figure 8**, the samples subjected to the tests generally present a heterogeneous rock texture consisting of claystone levels and anhydrite veins and layers of different frequencies. The thickness and elongation of the calcite veins in the claystone levels range from mm to cm. Its mineralogical composition is

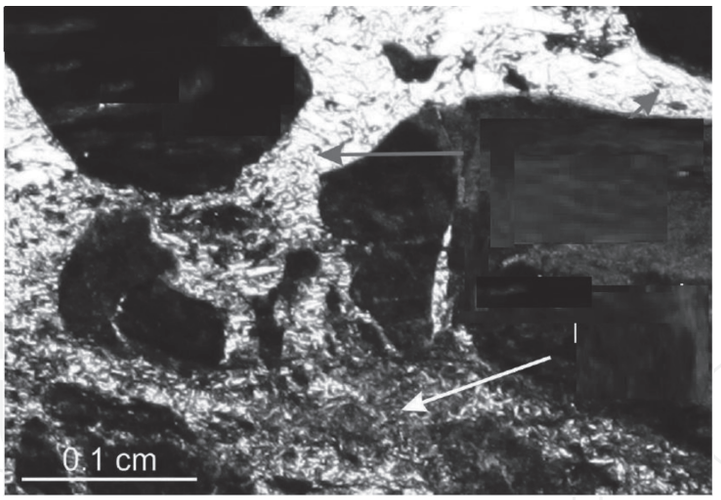

Figure 8.
Different chlorite shale matrices according calcite to shale content.

generally composed of anhydrite and clay minerals. Typically, the clay content and anhydrite content are inversely proportional to the samples. In other words, samples with low clay content generally contain higher density calcite veins.

Changes in the microstructure and mineralogy of the clay matrix, which appeared homogenous macroscopically, were determined in the microscopic examination of the samples subjected to experiments. As seen in **Figure 5**, the brown, dark brown and black regions usually contain clay matrix and rarely scattered calcite lumps in it. The areas seen in more gray tones form fine-grained anhydrides dispersed in fine-grained clays and form calcite-rich clay matrix. The anhydrite content and distribution in the clay matrix varies in sections. Besides, different types of matrix can be found in the same example.

As a result of the experiments conducted under environmental stress conditions, it was determined that the highest strength values σ varied between 9 and 81 MPa depending on the mineralogical composition of the samples. Failures occurred along the clay matrix in samples with low uniaxial compressive strength values. The samples with high values σ are the samples containing more than 84% marl. The general images of these examples show a homogeneous structure. The uniaxial compressive strength values σ obtained were accepted as extreme values σ indicating the strength properties of marl veins and clay matrix. In cases where the clay content is more than 10%, the uniaxial compression strength decreases very little. The opposite situation develops when the clay content is less than 7–10%. In this case, uniaxial compressive strength increases significantly due to the relatively increasing marl veins.

After these results, the relations between mass distribution of clays and σc under uniaxial conditions are evaluated in **Figure 9**. The standard test results similar to the σ values were obtained in uniaxial compression strength were encountered. When the clay content is more than 7–10%, the σc values decrease with an almost constant orientation.

Thus, in conditions where the clay content is less than 7–10%, σc values τ show a significant increase with the decrease of the clay percentage. In view of these results, it is thought that the initial fractures were controlled by the mechanical properties of the claystone levels, as the claystone levels were weaker than the low calcite belt levels.

The presence of chlorite belts is shown in claystone matrices of different type belts and different anisotropic strength properties together in the same sample. In the slip area of Avgamasya Open Pit quarry No 2. shale face the sliding shale formations is shown in **Figures 10** and **11**.

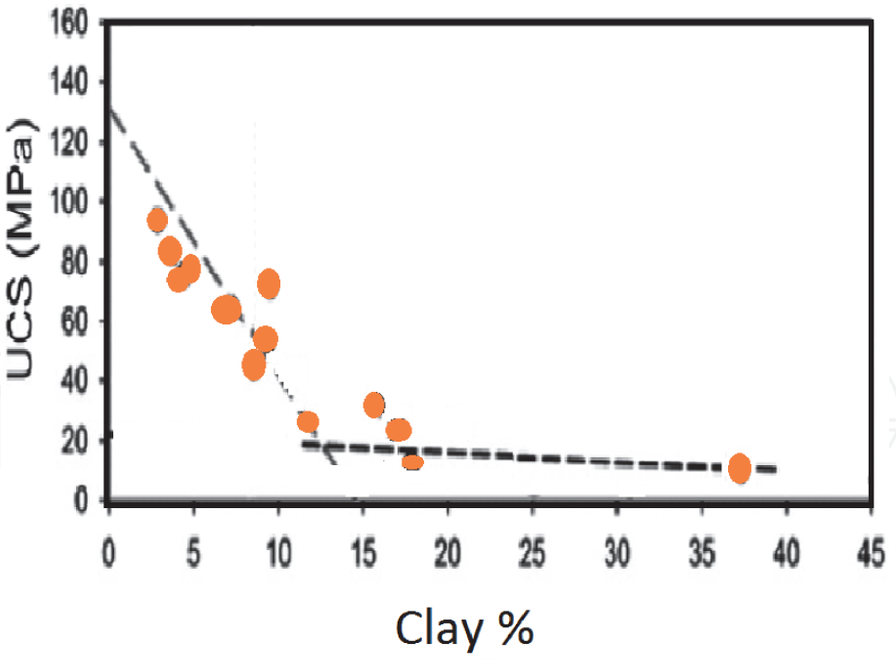

Figure 9.
Change of σ uniaxial compressive strength value according to clay content.

Figure 10.
Free rock slide and falling site in Şırnak Asphaltite open quarry No 2, satellite view 1/18000.

Figure 11.
Free rock slide and falling site in Şırnak Asphaltite open quarry No 2, free slide over excavation area, 1/1000.

3. Geotechnical studies

Stack weight in the slip area to determine the geotechnical stability in American Standards (ASTM and GEO5) based. In the area where the strengthening cabling of the masses and the presented soil rock interface of the phase content is given in **Tables 1** and **2**.

Slip face of shale and limestone rock pillar parameters are given in **Table 3** below.

Free slide rock stability to assess the risk of slipping GEO5 program used and was advantageous. Rock stability GEO5 program provided safety analysis at 1.35 safety factor. Stability analysis of weight slices as wide 3 m blocks as possible cut into slices. On Slope S1 free slip surface formed like 2m mesh using GEO 5 FEM program by groundwater data section submerged discharge gave the critical red

Sample No	Asphalt Ash compost fill	Asphalt+Fine Shale compost fill	S1	S2	S3	S4
height(m)	800	850	925	921	933	927
Wopt,%			15.90	13,70	10,80	11,40
c′(kpa)	52	88	0,52	0,59	0,63	0,55
φ′	24,2	22,5	32,50	22,50	21,00	20,00
L1(%)	11.8 Mpa σ	9.6 Mpa σ	26	15	28	17
P1(%)	42 RQD	40 RQD	19	11	18	22
Ip (%)	46 RMR	44 RMR	10	9	8	12
γs g/cm^3	2,70	2,70	2,40	2,50	2,40	2,30
Soil	zayıf	zayıf	SP	SP	SP	SP
$\gamma_{doğal}$ g/cm^3	1,94	2,14	1,82	1,76	1,90	1,70
γ_{kuru} g/cm^3 Kum ve çakıllı	1,94	2,14	1,65	1,6	1,78	1.60
γ_{doygun} g/cm^3	2,0	2,23	2,02	1,84	2,0	1,8

Table 1.
The samples taken from the slopes of the masses on the results obtained from the geotechnical testing.

Örnek no	S11	S21	S31	S41
γ_k max g/cm3	1,68	1,93	2,05	1,90
wopt %	15,9	19,0	12,3	13,0
Permeability (k) (cm/s)	$5{,}63*10^{-4}$	$6*10^{-4}$	$3{,}0*10^{-4}$	$5{,}62*10^{-4}$

Table 2.
Permiability of the samples taken from the slopes.

Specification of rock fill	Asphalt Ash compost fill	Asphalt+Fine Shale compost fill
Natural unit weight, γ_n (kN/m^3)	16	18
Saturated unit weight, γ_d (kN/m^3)	16	18
Cohesion, c (kN/m^2)	52	88
Intern. Friction Angle, ϕ (°)	30	34

Table 3.
Physical and mechanical properties of asphalt composite fill.

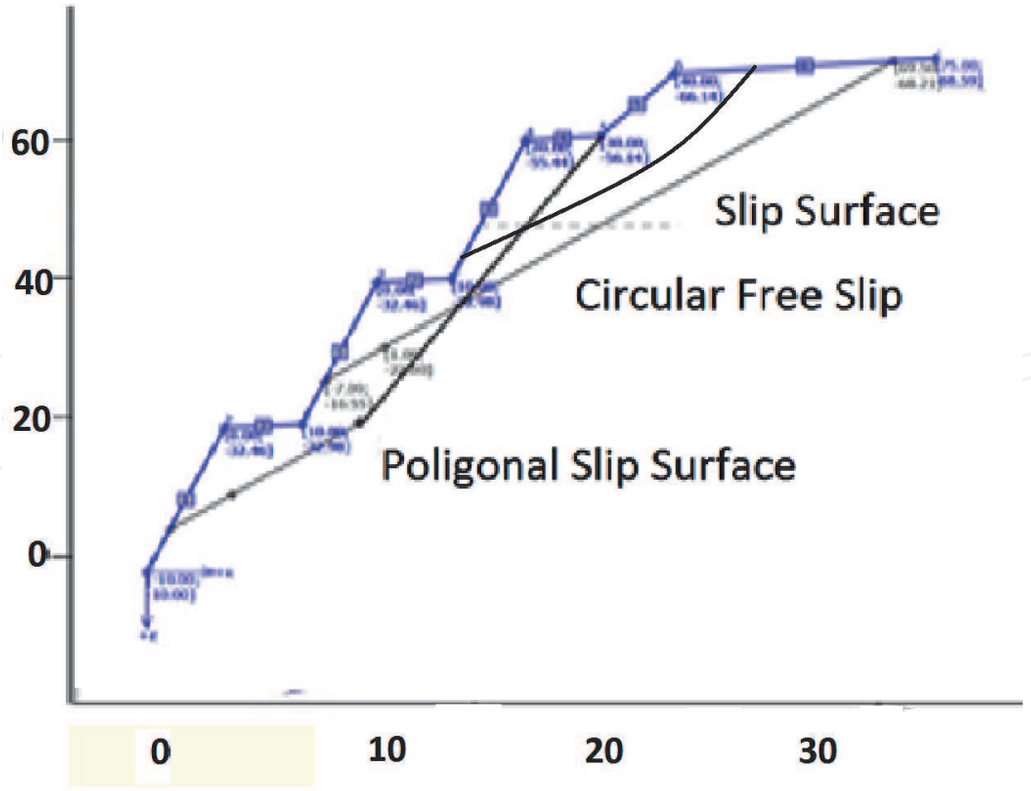

Figure 12.
S1 cross-section of rock slope of the study area, circular free rock sliding surfaces, sensitivity analysis rock stability using GEO5 program.

level slip surface effect and poor stability factor was practiced by lower mesh cross section [19, 20]. Using GEO5 on slip slice chart is advantageous at different slip surface pore pressure in program as in **Figure 12**, depending on the rock surface or planar wedge type drift is not formed in particular from 30 to 40 m length was determined.

Safety factor was in the ASTM standard as based GEO 5 rock stability safety factor of over 1.35. Using the parameters determined by model chart analysis of GEO 5, the appropriate support system for the long-term stability of the slopes was determined. Accordingly, it was decided to make asphalt cohesive support with fly ash material in front of the slope. Subsequently, 2 m long rock bolts were placed to provide short-term slope stability. After this stage, it was understood that a compost of asphalt-cover structure should be made on the crack section. The slope was required to ensure the long-term stability of the Asphaltite open pit quarry.

4. Slope analysis of S1 and S2 shale soil/rock face slopes

The stack S2 hillside after rains made the small size of the movements that have been identified in field studies. No. S2 to develop pile slope is covered with talus and 10 m mesh rock stability GEO5 programs were created problem due to heterogeneous structure and complexity with the program (**Figure 3A**). S2 The top of the stack and the maximum height difference between the heel point 45 m, the slope of the maximum height of 50 m, the slope of the surface tilt angle is 40°.

Regarding cohesive resistive parameters obtained from the asphalt composed rock formations made in c '= 1.9 kpa, φ '= 22°, $\gamma_{nat.}$ = 1.97 = 2.27 g/cm^3 g/cm^3, and are used to γ_{dry}. According to γ_{dry} and γ_{nat} calculated separately on the potential slip surface deformation iso values seen in **Figure 13**.

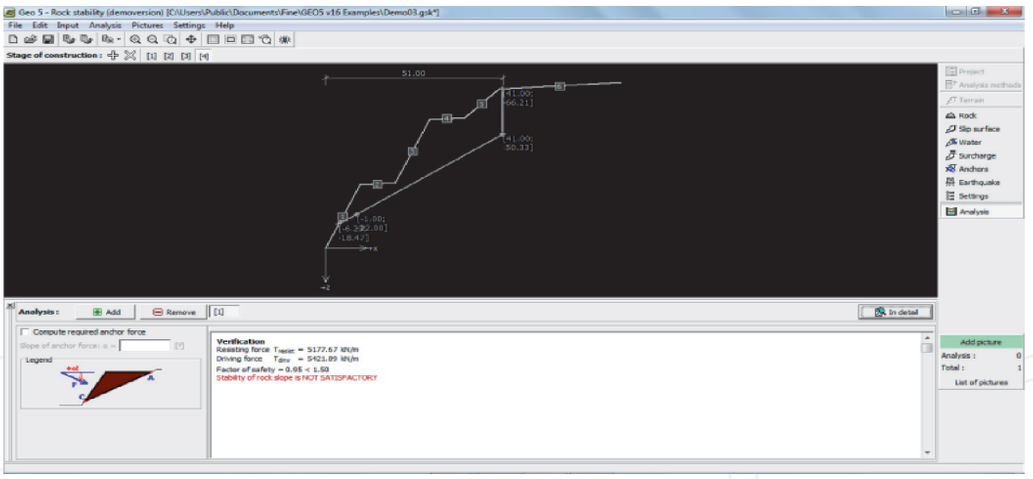

Figure 13.
S1 section of the study area slopes 10 m slice topology, b. Deformation rock stabilty stability analysis GEO5 programs, cut red 30 mm unstable displacement.

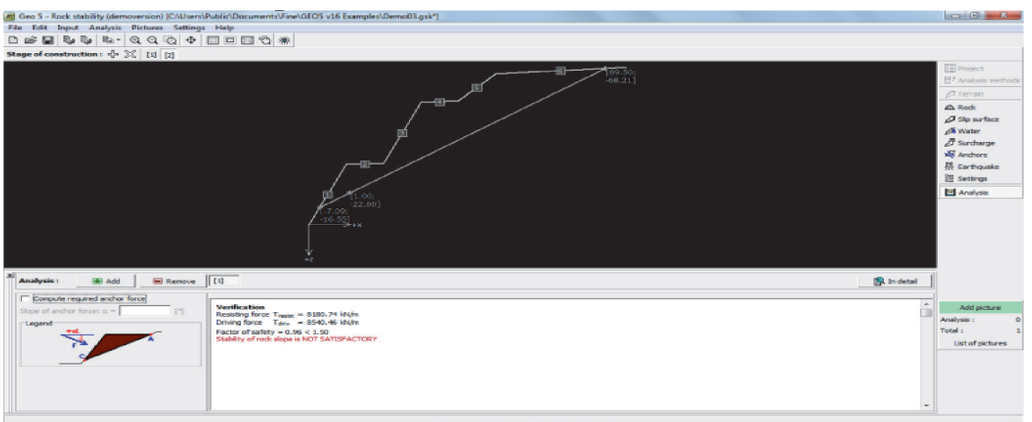

Figure 14.
S2 section of the study area slopes 10 m slice topology, b. deformation rock stabilty analysis GEO5 programs, cut red 30 mm unstable displacement.

S2 after water perched table on the slope of a deep instability, high shear force occurred. The instability was observed. Similarly the slope S3 indicates instability and displacement reached 30 m depth slip circular surface in Bishop Theory. (**Figure 12**)

In addition, 1 m wide and 10 m high pillar construction by cable cover by a safety factor values were above 1.5 (**Figure 14**)

When using a pillar to reduce instabilities under perched water tables in the slip deformation displacement was shown in **Figure 8** and displacement m below the maximum possible shift of the substrate reached 9 m depth.

The rock and filled asphalt waste fly ash compost shear stability ranged from 10 to 13 kPa with 610 kPa reaching a possible shift in the base.

5. Results and discussions

Therefore, the existing design was updated in this way and the safety coefficient of the slopes was obtained over 1.5 when the asphalt cohesive support structure was filled with 2 m filling as seen in **Figure 4**. As a result, the long-term security conditions of the shale slopes could only be achieved with these suggested measurements. and pillar cabled support. Cracks occurring in the S1 S2 and S3 slope as

seen in **Figure 2** reflected the free sliding situation where the safety coefficient was below 1 for 2 m blocks. For the stabilization case where the safety coefficient was over 1.35, the slip surface water parameters of the rock material on the slip surface were determined by slice weight analysis. Since the proposed analysis method was available for anchorage rock slopes, GEO 5 was directly used in this study. Because it was clear that completely degraded shale forming a weak slope over asphalt filled stabilized rock mass or completely free slip ground. GEO 5 method was preferred as the most suitable method for characterization of the free stability of the slope. RocScience software was also using finite element mesh programs and the parameters at this case of complete failure were determined. GEO5 analyzes were performed using the slice method. In this method, the safety coefficient is obtained by decreasing the shear strength parameters of the material forming the slope. GEO5 program calculated the 1.35 safety coefficient using shear force and resistive load. The reduced resistive load reduction method produced slide on slice weight principles. On the effective pore pressure, the rock failure by shear performs on below Eq (23).

$$\sigma'_1 = \sigma'_3 \cdot \frac{1 + \sin\varphi}{1 - \sin\varphi} + 2 \cdot c \cdot \frac{\cos\varphi}{1 - \sin\varphi} \tag{23}$$

As a result of analysis, shear resistive work performed in the field of geotechnical stabilization, the future should be considered a danger to very large fills and the filling cracked field should be determined according to the method of stabilization. Also within the project study area will be opened due to urban use preventive methods to investigate the instability in the region and it is important to develop a separate.

The stability was increased by compost rock cracks filled with asphalt/fly ash density reducing the water sorption content of uniaxial test blocks for 25 volume % rock cavity by 85% asphalt and 15% fly ash filling as shown in **Figure 15**.

The uniaxial compression strength of shale was increased to over 9 MPa by compost rock cracks filled with asphalt/fly ash density reducing the water sorption content of uniaxial test blocks for 25 volume % rock cavity by 85% asphalt and 15% fly ash filling as shown in **Figure 16**.

The uniaxial compression strength of shale was decreased to lower 8 MPa by compost rock cracks filled with increased fly ash content increasing the water sorption content. The uniaxial compression strength decreased to lower values in

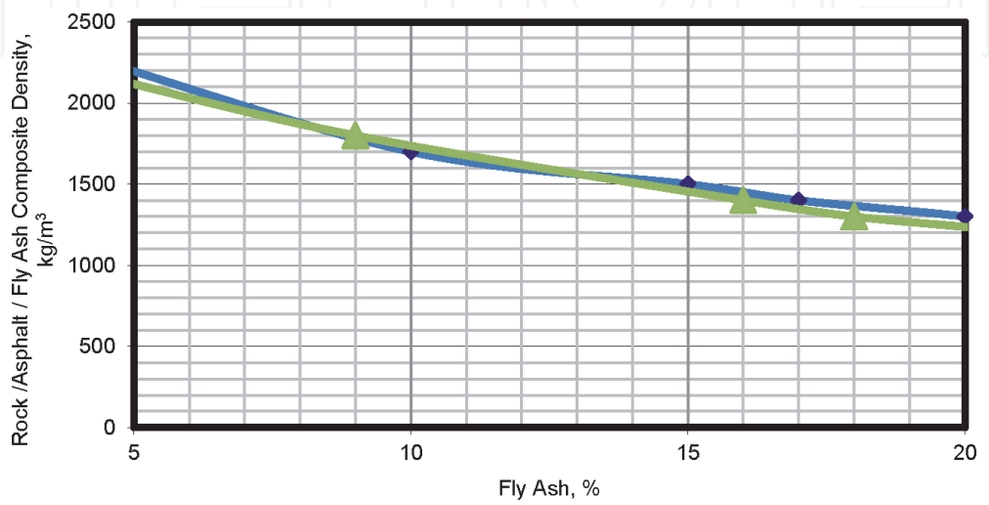

Figure 15.
The Bulk Density of the asphalt/fly ash filled Rock composite regarding Fly Ash Addition Vol%.

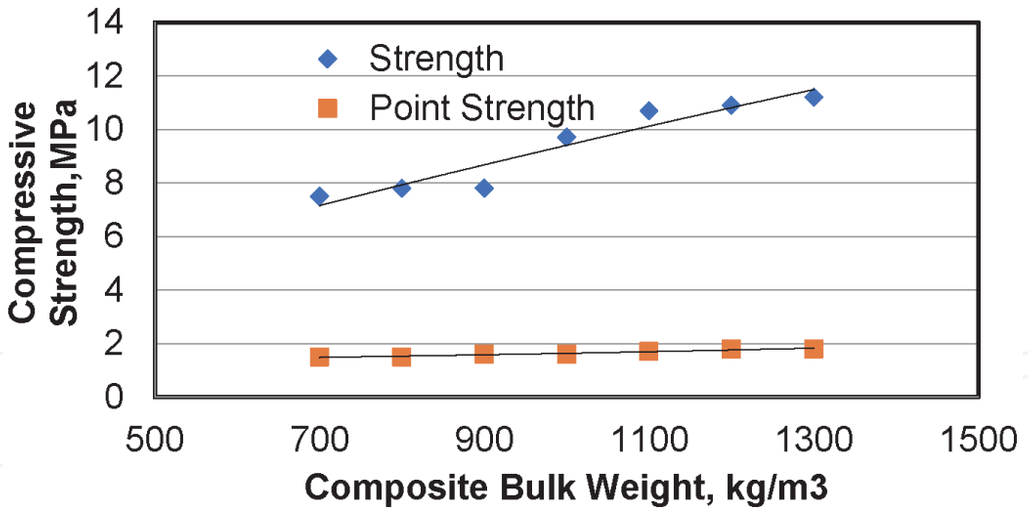

Figure 16.
The Compression Strength and I_s of the asphalt/fly ash filled Rock composite regarding Bulk Weight.

tested blocks for 25 volume % rock cavity by 80% asphalt and 20% fly ash filling as shown in **Figure 17**.

The water saturation of shale tested blocks was decreased over 70% by compost rock cracks filled with increased asphalt content over 60 vol % with increasing the cohesive filler content in tested shale blocks for 25 volume % rock cavity as shown in **Figure 17**.

In the scope of this study, both the numerical analysis and the proposed new asphalt flay ash fillings were evaluated for the reinforcement of free slides and stabilization of the migrating slope excavation, as well as the necessary weight slice analyses by GEO5 to ensure slope stability in the case sections of Avgamasya Pit Quarry No 2. The asphalt filling performance for free rock sliding was managed for slopes S1 S2 and other critical sub water perched face as seen in **Figure 3** caused water filled cracks and weak sub face soil texture.

5.1 Stabilization work and free sliding land and asphalt crack fill study

As a free slide soil -shale slip type was driven possible in rock falls of 2–5 m facing slopes, the main concepts of asphalt flay ash mixture filling was considered for stability and reinforcing weight slices over analyzed slip surface as explained above. Here, the rock cohesion was improved as an isolated block between water

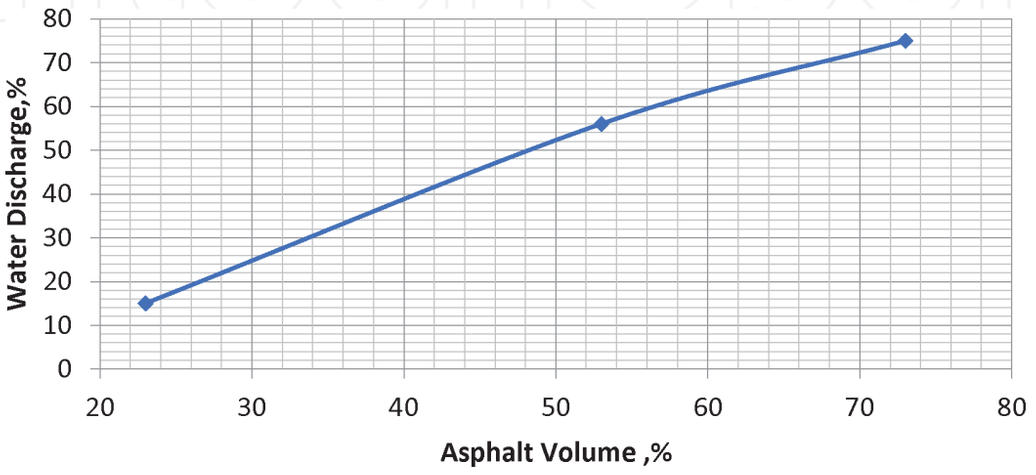

Figure 17.
The Water discharge of the asphalt/fly ash filled Rock composite regarding Asphalt Weight.

planes. The critical slopes were investigated that this block will not slip on planes with certain friction coefficients by improved cohesive matter of asphalt bound filling. The most important part of the problem was to determine the numerical values of crack filling performance by asphalt ash mixture that characterize the region in the stabilization analysis based on this theoretical idea. Numerical values of cohesion in stability problems determined by crack discontinuity. It can be summarized as the orientation of the surfaces, the average friction coefficients between these surfaces, the dimensions of the sliding wedge and the crack water pressures between the surfaces. Since these asphalt bound composite rocks were tested in various measuring techniques, the stability analysis of a rock slope should be done within the maximum and minimum cohesion values of these binder compost properties. The smallest of the safety numbers to be obtained should be used in the reference sizing, by the extensometer wire measurements as seen in **Figure 18**.

The rock fall, 3 m length crack elevation, asphalt compost filling made difference between the top and the heel point on 15 m. 30 m maximum height of the slope. The frequency distributions of the discontinuity orientations in the region are obtained in the form of a contour diagram as a result of placing a large number of discontinuity orientation measurements in a co-area network and a certain statistical evaluation. From this diagram, the maximum frequency orientations are called the dominant discontinuity orientations and they determine the planes to be used in stability analysis (Eq. (7)).

The mechanical properties of these discontinuity planes in terms of the stability of the rock slopes were free failures and friction coefficients. These properties can be determined as a result of shear tests of samples with discontinuity taken from the field. The Friction matter was critical in shale slopes due to low friction angle of below 22°. The force required to slide a block weighing W on a horizontal plane in a direction parallel to the plane must exceed the co-failure and friction force between the two surfaces. If the cohesion between two surfaces is assumed to be zero, the force required for shear should be W tgϕ,n weight slice chart. (**Figure 19**). The shear driving force reduced by strength planar levels auger bored and asphalt fill - wire net anchorage were applied as seen in **Figure 19**.

The free slip motion, shear forces in a slope was varied depending on the volume of the mass that is able to slide. Accordingly, the shape and therefore the weight of the mass that can slide should be found. In order to perform this procedure, it is necessary to know the properties of the mass that can slide and to be included in one

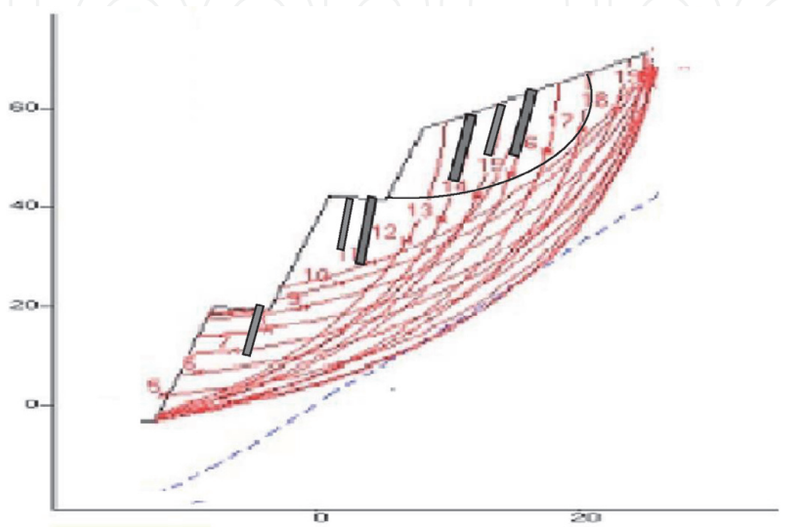

Figure 18.
Asphalt Crack Landfill Application cross-section on hazardous free slip area.

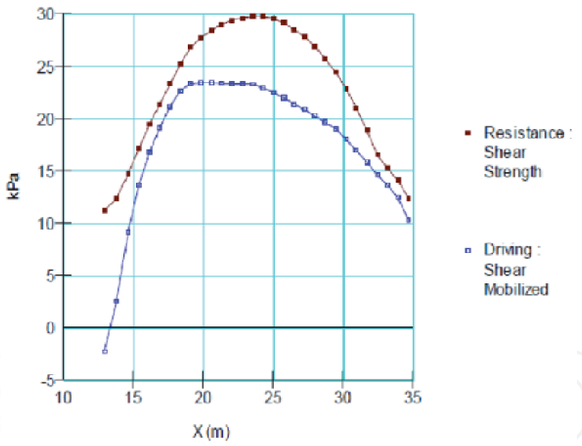

Figure 19.
Free slide shear load and driving forse over slice of slip surface on the base of water saturation of rock/ AsphaltComposite.

of the rock or ground class. Since the soil rock facing slip grounds was considered as heterogeneous, continuous and mostly anisotropic, and the mechanical properties of rocks, which had a discontinuous environment, and therefore the slice method was considered to be applied in even those free rock falls. It was impossible to apply the stability analysis model methods for rock falls applied to the open pit mines and road slopes of the heavily cracked rock slopes with the thought that the material itself was cut during the slope deterioration. Although The free soil slide was occurring with weight slice Bishop methods at 50–60 m length, the rock free slide was calculated for this shale formation so that a vertical limestone slope was fallen down at a height of 7–8 m That was the most common case to be broken as well in the past.

Although the idea of rock blocks sliding on a plane in rock slopes is an element, it is seen that rock wedges (weight blocks) bounded by two or more surfaces are formed as a result of the intersection of various discontinuities in nature, and their stability is more common in engineering works. In such cases, the rock wedge can slide, not on a plane, but on two planes, and its movement can be in the direction of the intersection of two planes. If it is, the event may occur.

The asphalt composed landfill of cable anchorage slopes developed cohesive resistivity and decreased perched water level on free sliding surfaces and the safety factor values reached over 1.5 and 1.8.

6. Conclusions

Asphaltite open pit mine and asphaltite excavation seam was hard to control against free sliding rock surrounding areas. There were 60 m even higher steeper slopes at angles over 65°. There were sliding large land marly shale masses or shattered shale rock formations. Underground water and harsh climatic conditions contain high risk hazard areas in operation site with higher risk factor of free slide. In order to eliminate rock falls and related events, significant precautions should be taken. The rock fall risk may ease to take precautions using asphalt composite filling. Even the application of elimination rock falls by wire net may reduce water content of soil. In this research, the pillar of 3 m and wire net were used with stabilization. The stability mixture of asphalt fill at certain thickness of 20 mm increased the safety. The low strength and porosity was critical for slide. The hazardous area could be safer by cohesive asphalt bound of rock cracks and long free rock slip surfaces out of water pressure.

Rock samples performed on the laboratory test results in the slope material not permeable that the cohesion value of 54–184.7 kPa, angle of internal friction of the 30.5–32.4° varied among marly shale/limestone with standard classifications. Stability analysis performed in the models srowed in **Figure 5** were unstable free slide rock interfaces. By use asphalt stabilization and pillar the hazardous free sliding slopes were converted to the stable condition. Shear force causing free slide was redueed by asphalt flyash mixture filling by cohesion of 400 kPa and 2 MPa shear strength with rock at 19 MPa uniaxial strength.

High strength landfill mass improved the slope stability. However, low strength foam concrete landfill might result in higher water discharge and drier soil condition. The pillar bottom layers avoided water saturation of cracks and slip surface bottom area even sequential top surfaces of slopes.

Dissociation detailed inclinometer observations provided in rocks on free slide area also offered a positive contribution to stability problems.

For those reasons, asphalt composite crack fill can use virtual any classical slope stability programs, rock slope stability calculations in order to do construction safety and dry soil matters as given factor over 1.35.

Symbols

c ‘kg/cm^2	Effective Cohesion
c kg/cm^2	Cohesion
Φ’o	Effective internal friction angle
Φo	Internal friction angle
τ kg/cm^2	Shear stress
σ kg/cm^2	Normal stress
Ip	Plasticity index
Ll	Liquid limit
Pl	Plastic limit
Wopt	Optimum water content
γNatural g/cm^3	Natural unit volume weight
Saturated g/cm^3	Saturated unit volume weight
γDry g/cm^3	Dry unit volume weight
γkmax g/cm^3	Maximum dry unit volume weight
γs g/cm^3	Grain unit volume weight
k	Permeability coefficient
S1, S2, S3, S4	Şırnak free slide slopes no. 1, 2, 3, 4
S11	Sample taken from Şırnak Asphaltite Open Pit Mine free slide slope no.
SP	In the combined ground classification; poorly graded sand, gravel sand, fine material no
SW	In combined ground classification; well-graded sand, gravelly sand, little or no fine material
SC	In the combined ground classification; claystone sand, sand-clay mixture
GW	In combined ground classification; well graded gravel, gravel-sand mixture, fine material little or no
J_i	Joint density sequence at slice i
N	Serial distribution of Discontinuity
R_c	Shear risk factor
F	Safety factor
σ	Compression Stress

$\tau_{\theta i}$	Shear Stress at slip surface at slice i
u	pore presssure

IntechOpen

Author details

Yildırım İsmail Tosun
Mining Engineering Department, Engineering Faculty, Şirnak University, Şırnak, Turkey

*Address all correspondence to: yildirimismailtosun@gmail.com

References

[1] Airey, G.D. and Collop, A.C., 2014, Mechanical and structural assessment of laboratory- and field-compacted asphalt mixtures International Journal of Pavement Engineering *Volume 17, 2016 - Issue 1: Asphalt compaction*

[2] Tashman, L., Wang, L. B. and Thyagarajan, S. 2007. Microstructure characterization for modeling HMA behavior using imaging technology. *Journal of Road Materials and Pavement Design*, 8(2): 207–238.

[3] Bieniawski, Z.T. 1967. Mechanism of brittle failure of rock Part I - Theory of fracture process. *I. J. of Rock Mech. and Min. Sc. and Geomech. Abstr.* 4: 4, s. 395-406

[4] Hoek, E. and Bray, JW, 1977, Rock slope engineering, Stephen Austin and Sons, Ltd., Hertford, 402 p.

[5] Lamp, W. T. and Whitman, RV, 1969, Soil Mechanics, John Wiley and Sons, New York

[6] Bishop, AW, 1955, The use of the slip circle in the stability analysis of earth slopes, Geotechnique, Vol. 5, 7-17.

[7] Hoek, E., 1970, Estimating the stability of excavated slopes in Opencast mines, Institution of Mining and Metallurgy, A105, A132

[8] Paşamehmetoğlu, LV, Özgenoğlu, A., Watermelon, C, 1991, Rock Slope Stability, 2 Print, T.M.M.O.B Mining Eng. Room Publications, Ankara, May.

[9] Anbalagan, R., 1992, Landslide hazard evaluation and zonation mapping in mountainous terrain, "Engineering Geology, 32:269-277,

[10] Fall, H, 1987, "Geotechnical Developments", DSI slope of the Stability and Retaining Structures Seminar, Samsun

[11] Anonymous, 2011, Şırnak Provincial Administration Reports.

[12] Anonymous, c 2011, "Turkey Earthquake Zone Map", Disaster and Emergency Management Bureau, Earthquake Department Ankara

[13] ASTM D616-07, 2007.Standard test method for Fly ash materials and compositions, slag materials, ASTM, Pennsylvania

[14] ASTM C 330, 2013.Standart Specifications For Lightweight Aggregates for Structural Concrete, ASTM, Philadelphia.

[15] ASTM D6024-07, 2007.Standard test method for Ball Drop on Controlled Low Strength Materials, ASTM, Pennsylvania.

[16] ASTM C 136, 2013.Standard test method for Sieve Analysis of Fine and Coarse Aggregates, Pennsylvania.

[17] Anonymous, 2013, GEO5 programs - Engineering Manuals - Part 1 - Part 2 h ttp://www.finesoftware.eu/geotechnical-software/

[18] Anonymous, 2009, GEO5 programs - FEM - Theoretical Guide http://www.finesoftware.eu/geotechnical-software/

[19] Görög P & Török, A, 2007 Slope stability assessment of weathered clay by using field data and computer modeling: a case study from Budapest, Natural Hazards and Earth System Sciences, 7, 417-422, www.natu-hazards-earth-syst- sci.net

[20] Görög P, 2006, Stability problems of abandoned clay pits in Budapest, IAEG 2006, Paper number 295, The Geological Society of London

[21] Dramis, F., Sorriso-Valvo, M., 1994 "Deep-Seated gravitational slope

Deformations, related landslides and tectonics", Engineering Geology 38, 231-243,.

[22] Hoek, E., 2013. Practical Rock Engineering, notes by Evert Hoek Hoek. My http://www.rocscience.co

[23] Hutchinson, JN., 1995 "Landslide hazard assessment. Keynote paper. In: Bell DH (ed) landslides, Proceedings of 6th International Symposium on landslides ", Christchurch, New Zealand, vol 1 Balkema, Rotterdam, pp. 1805-1841,

[24] Kilic, R., Ulamış, K.., "Gölbasi (Ankara) Investigation of Mass Movements in the South," Bulletin of Engineering Geology, Engineering Geology Of Bulletin, Issue: 20 (75-86).

[25] Prusa, J., 2009, Comparison of geotechnic softwares - Geo FEM, Plaxis, Z-Soil, XIII to ECSMG, Vanicek et al. (Eds). cgts, Prague, ISBN 80-86769-01-1, (Vol. 2)

[26] Vaneckov, V, Laura J, J Prus, 2011, Sheeting Wall Analysis by the Method of Dependent Pressures, Geotec Hanoi - ISBN 978 - 604-82 - 000 - 8 ID No. / Pp. 7

[27] Wiley, L., 1987 "Stability Slope and Geomorphology Geotechnical Engineering", England,

[28] Tosun, Y. İ., Cevizci, H., Ceylan, H., 2014, Landfill Design for Reclamation of Şırnak Coal Mine Dumps - Shalefill Stability and Risk Assessment, ICMEMT 2014, 11-12 July 2014, Prag, Chekoslovakia.

[29] Tosun, Y. İ., 2014, A case study on use of foam concrete landfill on landslide hazardous area in Şırnak City Province, XX Congress of the Carpathian Balkan Geological Association, Tirana, Albania, 24-26 September 2014.

[30] Tosun, Y. İ., 2014, *Shale stone and Fly ash Landfill Use in Land-slide Hazardous Area in Sirnak City with Foam Concrete*, GM Geomaterials Journal, Vol 4, issue 4, pp 141-150 DOI: 10.4236/gm.2014.44014

[31] Yıldırım İ.Tosun, 2016, Kalker, Marn ve Şeylin Sünme Karakterizasyonu - Bitümlü Gözenekli Agrega için Don - Mikrodalga Kurutma-Bilya Darbe Dayanım Testi ile Sünme Etüdü, AGGRE 2016, 8th Internatıonal Aggregates **Sy**mposıum, October 5-7, Istanbul, Turkey

[32] Tosun, Y.İ., 2016, Use of Modified Freeze-Drop Ball Test for Investigation the Crack Propagation Rate in Coal Mining- Case Study for the Şırnak Asphaltite Shale, Marly Shale and Marl in Şırnak Coal Site, *IBSMTS 2016, 1th Internatıonal Black Sea Symposium on Mininig and Tunnelling*, November 02-04, Trabzon, Turkey.

[33] Moulia, M., Khelafib H., 2008. Performance Characteristics Of Lightweight Aggregate Concrete Containing Natural Pozzolan, *Building and Environment* , 43, s. 31–36

[34] Park, C. K. Noh, M. H. Park, T. H. , 2005. Rheological Properties Of Cementitious Materials Containing Mineral Admixtures, *Cement And Concrete Research*s 842-849

[35] Olard, F. and Perraton, D. 2010. On the optimization of the aggregate packing characteristics for the design of high-performance asphalt concretes. *Road Materials and Pavements Design*, 11 (Suppl. 1): 145–169. doi:10.3166/rmpd.11hs.145-169

[36] Tashman, L., Masad, E., Peterson, B. and Saleh, H. 2001. Internal structure analysis of asphalt mixes to improve the simulation of superpave gyratory compaction to field conditions. *Journal of the Association of Asphalt Paving Technologists*, 70: 605–645.

[37] Török, Á. Bögöly, G., Czinder, B.. Görög, P, Kleb, B.& Vásárhelyi, B., Lovas, T. Barsi, Á., Molnár, B., Koppányi Z. & Somogyi, J. Á., 2016, Terrestrial laser scanner aided survey and stability analyses of rhyolite tuff cliff faces with potential rock-fall hazards, an example from Hungary, Eurock 2016, Cappadicia, Volume: 877-881

[38] Á Török, Á Barsi, G Bögöly, T Lovas, Á Somogyi, and P Görög, 2017, Slope stability and rock fall hazard assessment of volcanic tuffs using RPAS and TLS with 2D FEM slope modelling, Nat. Hazards Earth Syst. Sci. Discuss., doi:10.5194/nhess-2017-56, 2017